On acoustic gunshot localization systems

Conference Paper · November 2015

CITATIONS
0

READS
792

1 author:

António Luiz Lopes Ramos
University College of Southeast Norway
24 PUBLICATIONS **81** CITATIONS

SEE PROFILE

SDPS-2015
Printed in the United States of America, November, 2015

ON ACOUSTIC GUNSHOT LOCALIZATION SYSTEMS

António L. L. Ramos
Buskerud and Vestfold University College
Faculty of Technology and Maritime Sciences
antonio.ramos@hbv.no

ABSTRACT

Automatic gunshot detection and localization systems have gained popularity in recent years, both for police and military use. The capabilities of such systems have been gradually improving as new techniques emerging from research laboratories are incorporated into the design. A gunshot event produces characteristic acoustic and electromagnetic signatures containing sufficient information to estimate the trajectory of the bullet and, ultimately, the shooter's location. This paper provides an overview of acoustic based gunshot detection and localization systems. Propagation models for both the muzzle blast and the shockwave are discussed, and three specific problems related to the processing of gunshot acoustic signatures are addressed: direction-of-arrival (DOA) estimation, noise cancellation, and issues related to multipath propagation.

INTRODUCTION

Automatic sniper localization devices have gained popularity in recent years with application in civil protection, law enforcement, and support to soldiers on missions where enemy snipers pose a serious threat. Locating highly trained enemy snipers using traditional methods based on human senses is very inefficient and might require more than one attempt. This is usually enough to allow the sniper to exit the local or simply move to a different spot and continue to cause casualties before getting away. Some examples of commercially available sniper localization systems include:

- BBN Boomerang (BBN Technologies, n.d.): an acoustic sniper detection system that uses an array of seven microphones. The system has been deployed by U.S. forces in Iraq and Afghanistan;
- REDOWL (REDOWL, n.d.): Sniper Detection System equipped with infrared camera, acoustic system, and laser range finder that aims at the source of the acoustic event.
- WeaponWatch (WeaponWatch, n.d.): a system claims to be able to detected weapons fire signatures for small arms, sniper rifles, machine guns, Rocket-Propelled Grenades (RPGs), Man-Portable Air-Defense systems (MANPADs), tanks, mortars, artillery, and others;
- ShotSpotter (ShotSpotter, n.d.): a system primarily designed for wide-area acoustic surveillance.

Strictly speaking, sniper localization systems are passive devices designed to detect and locate enemy snipers. The beginning of the interest in the topic can be traced back to the early 1990's and was pioneered by countries like the United States of America, Russia, France, and Canada. The primary objective is to develop automatic surveillance systems that can be useful to both police and military forces. But, despite recent advances in the field, there is still a long way to go towards making these devices more efficient, reliable, and capable of delivering a good performance under adverse conditions. As will become clear from the following discussion, there are multiple possible approaches to addressing this problem, depending on what kind of gunshot signatures (electromagnetic, acoustic, or even a combination of both) one chooses to process.

This work is concerned with the problem of designing acoustic sniper localization systems where the sniper's location is estimated by processing acoustic signatures associated with the firing of a gun, namely the muzzle blast and the ballistic shockwave. Issues related to noise cancellation, direction-of-arrival (DOA) estimation, multipath propagation, and algorithm implementations have been investigated and results have been reported in a number of earlier publications by the author himself and collaborators. Important contributions by other authors are also referenced where appropriate.

THE SNIPER LOCALIZATION PROBLEM

A sniper can be defined as any concealed gunman firing a rifle (Plaster, 2006). Police and military snipers are usually highly trained individuals working in teams of two members that, when on mission, have each a very specific but interchangeable task: spotting and sniping. Snipers can target or be targeted by other snipers with or without equivalent training. In conventional military situations it can take several days before the threat posed by an enemy sniper is eliminated, simply because skilled snipers are also experts in remaining invisible to their foes. Modern technology applied to this problem has the potential to hasten the process of localizing a sniper reducing the time to less than two seconds after a gun has been fired. In some cases, the presence of an enemy sniper can be detected even without a single shot has been fired (Plaster, 2006).

The detection and positioning processes can be based on different technologies depending on what kind of signature, acoustic or electromagnetic, is processed. The former, referred to in this text as acoustic sniper positioning systems,

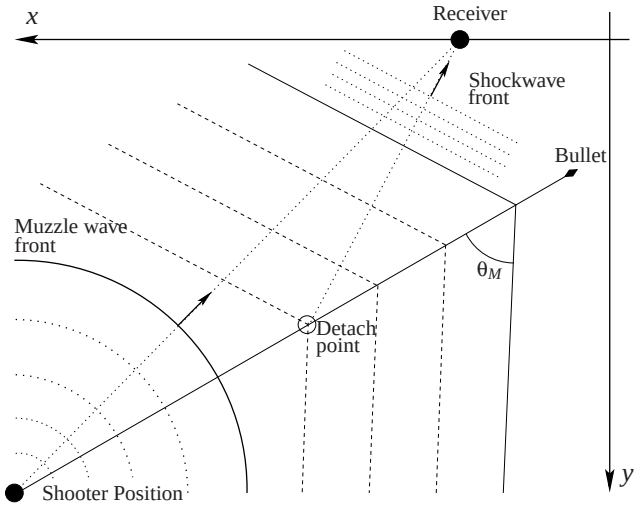

Fig. 1. A typical configuration for gunshot recording. θ_M is the Mach angle, and varies inversely proportional to the bullet velocity.

is based on the processing of the muzzle blast and the ballistic shockwave signatures, whereas the latter can be based on the processing of infrared signatures or lasers (Kastek, Dulski, Trzaskawka, Sosnowski, & Madura, 2010). Laser-based counter-sniper systems are not strictly dependent on the occurrence of a gunshot event. A few decades ago, the USA and Russia worked independently on laser-based sniper localization system that could detect and engage enemy soldier by neutralizing any telescope or night vision device in range. As described by Major John Plaster in (Plaster, 2006), these devices were designed to emit a visible laser beam powerful enough to blind enemy soldiers wearing night vision devices or using scopes. Later, the U.S.A. government reconsidered and decided to deploy its version of the laser-based sniper localization system without the engaging functionality (Plaster, 2006).

ACOUSTIC SNIPER POSITIONING SYSTEMS

Acoustic Sniper Positioning Systems rely solely on the detection of the muzzle blast and the shockwave acoustic signatures to estimate the position of a potential enemy sniper. There are also mechanically originated sounds, associated with the trigger, the hammer, and ejection of spent cartridges, which are detectable only if a sensor is placed in the proximity of the gun. These events are useful in forensics analysis (Beck, Nakasone, & Marr, 2011a; Brustad & Freytag, 2005), but are of no special interest in the design of sniper positioning systems. For this reason, they are not further considered in this work.

Figure 1 illustrates a typical configuration for recording of gunshot acoustic signatures. The localization process consists of three steps: (1) Detect the shockwave and the muzzle blast acoustic signatures; (2) Estimate their respective direction-of-arrival; and (3) Estimate the Mach angle of the ballistic shockwave and triangulate to finally find the shooter's location. The problem is that these two signals are not always present or easily detectable. This is related to a number of reasons, e.g., low signal-to-noise ratio due to additive background noise, and multipath propagation that results from reflections at the surface of buildings, mountains, or even the ground. These issues are further discussed in the remaining sections of this work.

The Muzzle Blast

The muzzle blast is a consequence of the sudden expansion of gas following the explosion in the gun barrel. The generated acoustic energy is directly proportional to the volume of gas flow rate (volume velocity) at the source and propagates at the speed of sound. The speed of sound depends on the properties of the medium through which it propagates. In air, for example, it varies with temperature according to (Maher, 2007)

$$c = c_0\sqrt{1+\frac{T}{273}}, \tag{1}$$

where T is the air temperature in degree Celsius and $c_0 =$ 331 m/s is the sound velocity at $T = 0$ °C. This gives, for example, a propagation velocity of 343 m/s at a temperature of 20 degrees Celsius.

Although the acoustic energy radiates in all directions, the sound pressure is highest in the direction the gun barrel is pointing to. The cause of the attenuation measured in the rear sound pressure can be attributed mainly to the presence of the shooter's body and the physical characteristics of the firearm (Beck, Nakasone, & Marr, 2011b). The angular peak overpressure (radiation pattern) is, therefore, a function of the azimuth angle, ϕ, measured with respect to the line-of-fire. One of the proposed models for the angular peak overpressure is given by (Baker, 1973)

$$p(\phi) = P_{0^o}\left[1-\frac{P_{0^o}-P_{180^o}}{P_{0^o}}\sin\left(\frac{\phi}{2}\right)\right], \tag{2}$$

where P_{0^o} and P_{180^o} are the peak forward and rear pressures, respectively. Figure 2 illustrates the radiation pattern given by this model when P_{0^o} and P_{180^o} are set to 200 Pa and 120 Pa, respectively.

The source's sound pressure decreases exponentially with time and therefore the muzzle blast signal becomes very sensitive to additive background noise with increasing range. The rate of decrease depends on the flow characteristics of the source, but muzzle blasts can be generally described using the Friedlander equation (Beck et al., 2011b), a model for blast waves or explosions in air. Let P_0 and P_s denote, respectively, the atmospheric pressure and the peak overpressure generated by the muzzle explosion. The Friedlander equation can then be written as

$$p(t) = P_0 + P_s\left(1-\frac{t}{T_0}\right)e^{-bt/T_0}, \tag{3}$$

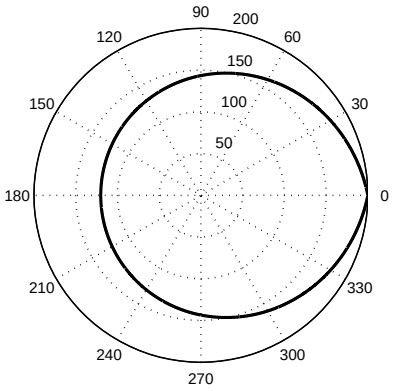

Fig. 2. Angular propagation model of the muzzle blast peak overpressure. Pressure values are in Pascal (Pa).

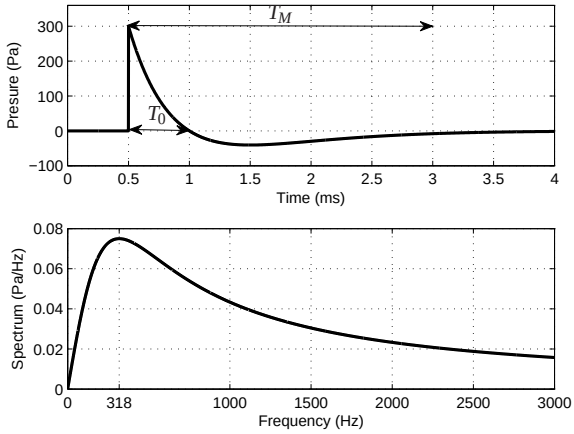

Fig. 3. Ideal time-domain signature and corresponding analytical frequency spectrum of a typical small firearm muzzle blast according to Friedlander's model. Setting $b = 1$, $T_0 = 0.5$ ms, with P_0 and P_s equal to 0 and 300 Pa, respectively, results in a total blast duration, T_M, of approximately 3 ms.

where T_0 is the positive phase duration and b is the rate of exponential decay. The analytical spectrum of the Friedlander's sound pressure model, obtained by taking the Fourier transform of (3), is given by

$$P(w) = \frac{P_s\left((b-1)+jwT_0\right)}{T_0\left(\frac{b}{T_0}+jw\right)^2}, \tag{4}$$

where w is the angular frequency (rad/s) and j is the imaginary unit. The corresponding magnitude spectrum, $|P(w)|$, is given by

$$|P(w)| = \frac{P_s}{T_0}\frac{\sqrt{(b-1)^2+T_0^2w^2}}{\left(\frac{b}{T_0}\right)^2+w^2}. \tag{5}$$

The magnitude spectrum in (5) has a peak at

$$w_{\max} = \frac{1}{T_0}\sqrt{-b^2+4b-2},$$

which is found by setting its gradient to zero and solving for w. Typically, small firearms muzzle blasts sound pulses last for approximately 3 ms, with a sound pressure level (SPL) of 140 dB (200 Pa) or higher (Maher, 2007).

Muzzle blasts are not always detectable, specially if sound suppressors are used or when the array of sensors is located several hundred meters away from the firing gun. In the latter case, due to propagation losses and additive background noise, the muzzle sound pressure may drop below the noise floor before it reaches the array of sensors, thereby resulting in increased difficulty in the detection process.

Figure 3 illustrates a theoretical small firearm muzzle blast modeled using the Friedlander's equation. In this example, the rate of exponential decay, b, was set to 1, the positive phase duration, T_0, was set to 0.5 ms, and the peak overpressure, P_s, was set to 300 Pa (144 dB). Replacing these values in (3) results in a blast duration, T_M, of approximately 3 ms, which is consistent with the duration of an actual small firearm muzzle blast.

The Shockwave

A ballistic shockwave, present only when the bullet is moving at supersonic speed, is characterized by a sudden rise in pressure followed by an approximately linear decline to a value nearly as far below as the original rise and then an almost instantly return to the atmospheric pressure (DuMond, Cohen, Panofsky, & Deeds, 1946). In reality, there are two different types of shockwaves involved: a compression shock and an expansion shock. In this work, the combination of these two events is referred to as a ballistic shockwave, or simply a shockwave. The shape of the time-domain representation of the shockwave resembles that of an "N" (see Figure 4a) and is sometimes referred to as the N-wave. In Figure 4, H and T stand for head an tail, respectively, and represent the peak positive and negative pressures caused by the head and tail of the bullet as it travels through the air at supersonic speed. The head discontinuity is also called an oblique shock when it is inclined with respect to the bullet trajectory, or a bow-shock when it is curved. The tail discontinuity is simply referred to as the trailing-shock.

The head and the trail discontinuities are separated by a small time interval, T', known as the period of the N-wave, that varies proportionally to the bullet length and the propagation time. The last holds because the two discontinuities H and T travel at different speeds. Specifically, the head and tail discontinuities travel at velocities slightly higher and lower than that of the local speed of sound, respectively (DuMond et al., 1946). This is illustrated in Fig-

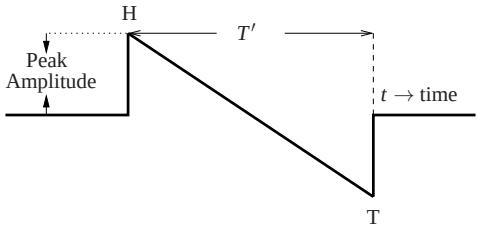

(a) The N-wave.

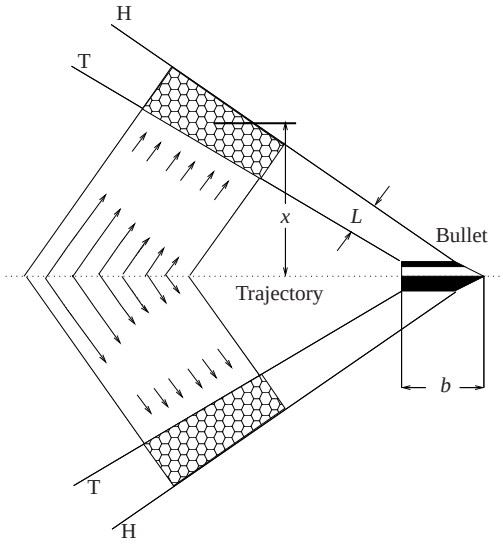

(b) Path of Energy transfer from bullet to shock wave. x: miss distance; L: wavelength.

Fig. 4. The Shockwave.

ure 4b, where the increase in the time interval T', separating the head and trail discontinuities as they propagate outwards from the bullet trajectory, is evident. Figure 4b also illustrates how the energy is transferred from the bullet to the shockwave. As the shockwave propagates through the medium, the average energy decreases and tends to dissipate relatively quickly due to three main factors: (1) increase in the mean radius **x**; (2) increase in the wave-length **L**; and (3) dissipation into heat.

In between the two main shock waves there can also be secondary compression and expansion shock waves. As these secondary shock waves propagate, they can merge into the main shocks waves or give rise to new shock waves if they have enough power (DuMond et al., 1946). By extrapolating this image (in a simplified version in Figure 4b) to the three-dimensional space, one can realize that the shockwave exhibits a cone shape involving the bullet trajectory, called the Mach cone. For this reason, the shockwave cannot be detected when the bullet is moving away from the sensor.

The angle of propagation of the shockwave with respect to the bullet trajectory, θ_M, referred to as Mach angle (see Figure 1), varies inversely proportional to the bullet velocity and is given by

$$\theta_M = \sin^{-1}\left(\frac{c}{v}\right) = \sin^{-1}\left(\frac{1}{M}\right), \tag{6}$$

where v and c are, respectively, the instantaneous bullet velocity and the speed of sound. It is common to use the terms subsonic and supersonic to refer to projectile velocities or flow speeds which are below and above the local speed of sound, respectively.

The ratio $M = v/c$ is a dimensionless quantity known as the Mach number, named after the Austrian physicist and philosopher Ernst Mach (1838-1916). The Mach number is often used in some disciplines, e.g., aerodynamics, to describe particular regimes. For example, $v = c$ results in $M = 1$, which corresponds to a Mach angle $\theta_M = \sin^{-1}(1) = 90^o$. This point, know as the sonic regime, is where shock waves start to form or vanishing, depending on whether v is increasing or decreasing. In fact, Mach numbers in the range $0.8 \leq M < 1.2$ characterize a regime known as the transonic regime, a transition phase between the subsonic regime ($M < 0.8$) and the supersonic regime ($1.2 \leq M < 5$). NASA defines additional regimes such as the low hypersonic regime ($5 < M < 10$) to account for aircraft speeds which are much higher than the speed of sound, and the high hypersonic regime ($M > 10$) to account for atmospheric reentry speeds.

When a bullet moves through the air at a velocity higher than that of the local speed of sound, there is an increase in the entropy of the air caused by: (1) a compressive shock wave that propagates at a supersonic velocity relative to the air ahead of it and at a subsonic velocity relative to the air behind it; and (2) an expansive shock wave that propagates at subsonic velocity relative to the material ahead of it, and at a supersonic velocity relative to the material behind it. This fact has important implications in the reflection of ballistic shockwaves and has been treated in (Ramos, Holm, Gudvangen, & Otterlei, 2013b). For the sake of completeness, however, an overview of this topic is presented in the next section.

THE MULTIPATH PROPAGATION EFFECT

The additive background noise and the multipath propagation effects are two central issues that cannot be overlooked in the design of acoustic sniper localizations systems. This section presents a brief discussion on the multipath propagation effect in gunshot acoustics, while the additive background noise problem is discussed in the subsequent section.

In multipath propagation environments, the received signal is composed of a direct-path signal, which is present only when there is an unobstructed line-of-sight from source to receiver, plus N scaled delayed copies of the direct-path signal. The scaling factor is frequency dependent and determined by the characteristics of the reflec-

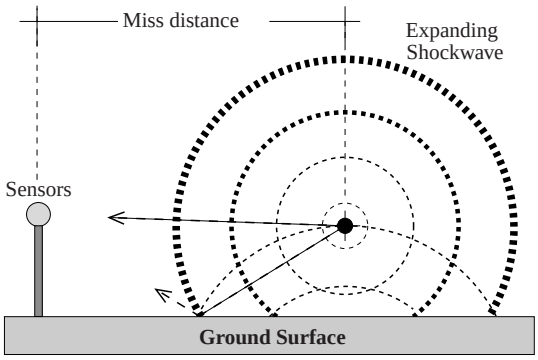

Fig. 5. Example of shockwave ground reflection. Bullet into paper sheet. Reader is at the sniper's position, and the muzzle sound travels in a strait path from reader to the sensors.

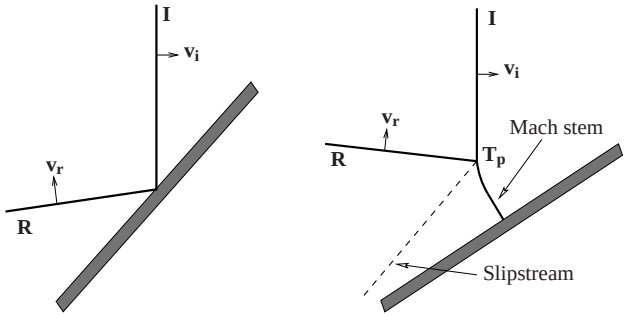

(a) Regular reflection. (b) Mach reflection.

Fig. 6. Main types of a moderate shock wave reflection. Legend: $\mathbf{I}\rightarrow$incident shock; $\mathbf{R}\rightarrow$reflected shock; $\mathbf{v_i}\rightarrow$velocity of the incident shock; and $\mathbf{v_r}\rightarrow$velocity of the reflected shock; $\mathbf{T_p}\rightarrow$ the triple point.

tive surface and the traveling distance, whereas the associated time-delay is determined by the propagation path and the respective angle-of-arrival. The multipath propagation effect poses less problems in open field environments, characterized by the absence of objects in the vicinity of the recording apparatus, but the analysis of recorded gunshot signals has shown that a shockwave ground reflection (please, see the illustration in Figure 5) is almost always present (Maher & Shaw, 2008).

The muzzle blast behaves like an ordinary acoustic pulse and thus its reflection at a given boundary follows the same principles governing the reflection of ordinary sound waves. Ballistic shock waves, however, are nonlinear phenomena and behave in a very peculiar way when reflecting off a surface. The first experimental study on the shock waves reflection phenomenon was conducted by Ernst Mach and published in 1878 (Mach, 1878). Mach identified two types of reflections: a regular reflection (see Figure 6a) that results in a two-shock configuration; and a three-shock structure, as illustrated in Figure 6b, which is nowadays referred to as the Mach reflection. The point where the three shock waves meet is called the triple point.

A new type of reflection, initially named the non-Mach reflection, was observed by von Neumann and would later be known as the von Neumann reflection (Semenov, Berezkina, & Krassovskaya, 2012). Today, shock wave reflections are classified into two main types: regular reflection and irregular reflections. Irregular reflections are believed to comprise several subtypes as recently reported by (Semenov et al., 2012). This topic is still receiving the attention of many researchers from different fields, e.g., fluid dynamics and solid mechanics (Ben-Dor, Elperin, Li, & Vasiliev, 1999; Brown, 2011).

In a ballistic shockwave reflection, two incident shock waves, one of compression and one of rarefaction, reach the boundary separated by the small time interval T', the period of the shockwave. The numerical analysis presented in (Jiang, Huang, & Takayama, 2004; Zhang, Liu, Chen, & Wang, 2012) shows that both regular and Mach reflections

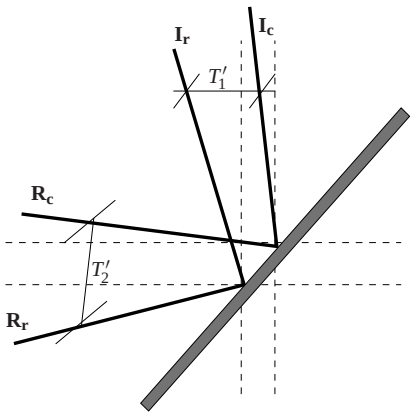

Fig. 7. Reference frame of a moving ballistic shockwave front reflecting at an oblique air-solid interface. Legend: $\mathbf{I_c}\rightarrow$incident shock of compression; $\mathbf{I_r}\rightarrow$incident shock of rarefaction; $\mathbf{R_c}\rightarrow$reflected shock of compression; and $\mathbf{R_r}\rightarrow$reflected shock of rarefaction; The period of the reflected shockwave, T_2', increases relative to the period of the incident shockwave, T_1'.

can occur in the case of shock waves induced by supersonic projectiles. As illustrated in Figure 7, a regular reflection of shock waves induced by supersonic projectiles, bullets in particular, can be regarded as a four-shocks configuration, comprised of: two incident shockwaves, one of compression followed by another one of rarefaction, plus two reflected shockwaves. As discussed by Ben-Dor et al. in (Ben-Dor et al., 1999), the two incident shock waves do not interact with each other at the boundary the same way they do when moving through the air. Indeed, the compression and rarefaction shock waves meet the reflecting surface at different angles of incidence altering the flow conditions at the reflecting surface and the relative speeds between the compression and expansion shock waves. Moreover, the period of the m-th reflected shockwave, T_m', measured at a given point in space will be greater than the period of the direct-path shockwave, T'. The increase verified in T_m' is therefore a consequence of two main factors, namely, the longer traveling time of the reflected shockwave, and the

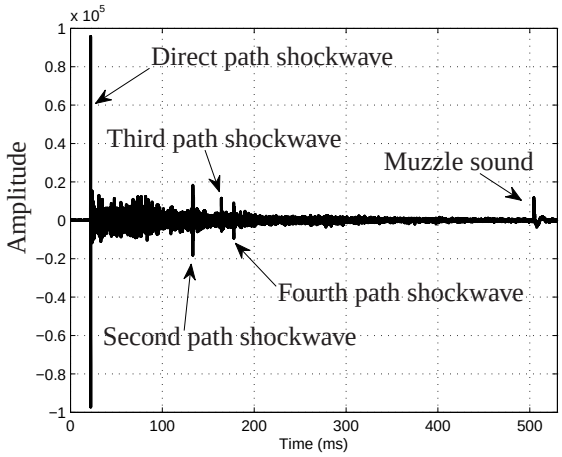

Fig. 8. Gunshot recording with reflections. The signal is upscaled by an exponential factor of $n^{3/2}$ during the first 83 ms, with n being the sample index. The scaling factor is kept constant from $t = 83$ ms on.

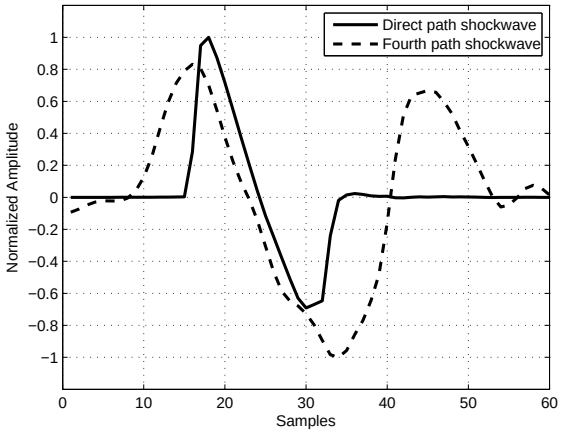

Fig. 9. Period of the direct-path shockwave versus the period of the fourth-path shockwave. Signals are normalized for better comparability.

interaction of the compression and expansion shock waves at the reflective boundary.

Figure 8 illustrates a typical gunshot acoustic signal recorded in a multipath environment. The signature belongs to a 12.7 mm bullet fired from approximately 540 meters with a passing distance relative to the sensors of roughly 62 meters. In this configuration, the power of the primary shockwave is much higher than the power of its reflections and the power of the muzzle blast. For a better visualization, the recorded signal was scaled using an exponential factor of $n^{3/2}$ during the first 83 ms, with n being the sample index. The scaling factor is kept constant from $t = 83$ ms on. As can be seen from the figure, the direct-path shockwave signal is followed closely by some reflections before the muzzle blast arrives.

Figure 9 compares the period of the direct-path shockwave with the period of the fourth-path shockwave. As can be seen, the period of the reflected shockwave has increased, as expected. This observation, in conjunction with the previous considerations about energy and spectral content made earlier, provide means to discriminate between direct-path and reflected shockwaves. This distinction is very important and can be used to increase accuracy in range estimation, thereby improving the performance and reliability of acoustic sniper localization systems, specially under multipath propagation which is characteristic of urban environments.

TECHNICAL ANALYSIS

Recall that the acoustic sniper localization problem can be divided in three steps: (1) Detect the shockwave and the muzzle blast acoustic signals; (2) Estimate their respective Direction-of-Arrival (DOA); and (3) Estimate the Mach angle of the ballistic shock wave and triangulate to determine the shooter's position. The whole process is obviously dependent on whether step one is carried out successfully, i.e., on whether the two acoustic signatures of interest are detectable. At the beginning of this research project, an algorithm that performs step three was already available and, therefore, it was decided that developing robust solutions to increase the reliability of the algorithms used in steps one and two should be a priority.

There is a combination of factors that can prevent the muzzle blast and the shockwave acoustic signatures from being properly detected. To begin with, both signals can be masked by the background noise. Indeed, considering the fact that the sound pressure is inversely proportional to the distance from the source, this is very likely to happen, specially in long range detection. The muzzle blast can also be suppressed at the origin if the gun is equipped with a silencer. As for the shockwave, the only way to guarantee its total absence is by using subsonic ammunition. Nonetheless, being able to detect the signals is a necessary but not sufficient condition for solving the sniper localization problem. For instance, the multipath propagation effect, discussed in a later section, can introduce ghost sources that make the localization problem even harder to solve.

NOISE REDUCTION METHODS FOR GUNSHOT ACOUSTICS

Adaptive filtering and spectral subtraction are two well known techniques that have been applied successfully to enhance signals corrupted by noise in a wide variety of scenarios. It was shown in (Ramos, Holm, Gudvangen, & Otterlei, 2012) and (Ramos, Holm, Gudvangen, & Otterlei, 2013c) that both methods can also be used for denoising of impulsive gunshot acoustic signals with satisfactory results. The *Least-Mean-Squares* (LMS) and the *Recursive Least-Squares* (RLS) are two popular families of adaptive filter-

ing algorithms with different properties concerning rate of convergence, stability, and computational complexity. The LMS algorithm is particularly known for its low computational complexity and stability. Nonetheless, in applications where higher rate of convergence and tracking capability are desirable, the RLS algorithm is a better option, specially in its stable array versions based on the QR decomposition. These benefits however come at a price of increased computational complexity of order $O[N^2]$. This fact motivated the development of the so-called fast QRD-RLS algorithms which have a computational complexity of $O[N]$, while exhibiting the same attractive numerical and convergence properties of the basic QRD-RLS algorithm. A detailed discussion on this topic can be found in (Ramos & Werner, 2009).

The spectral subtraction algorithm for denoising of gunshot acoustic signals, initially proposed in (Ramos et al., 2013c) and later on in an alternative version in (Ramos, Holm, Gudvangen, & Otterlei, 2013a), is a simple and effective method that offers some advantages, specially in terms of computational complexity. Another major advantage is related to the fact that these algorithms operate in the frequency domain. This aspect can be exploited when implementing feature extraction algorithms for signal recognition that usually requires frequency domain analysis as well. However, noise cancellation algorithms based on the spectral subtraction method have some known inherent limitations, e.g., amplitude and phase distortions, which cannot always be neglected (Evans, Mason, Liu, & Fauve, 2006). Nonetheless, the impact of these constraints becomes less relevant in applications where the resynthesized time domain version of the signal is not the primary objective. Another fundamental drawback of the spectral subtraction method has to do with the fact that it provides a very low SNR gain for input SNRs close to 0 dB and lower (Evans et al., 2006).

Array Processing Considerations

When an array of microphones is used, which is almost always the case, a DOA estimator that searches for the azimuth and elevation angles (ϕ, θ) that maximize the array's output power can be implemeted according to (Ramos, Holm, Gudvangen, & Otterlei, 2011)

$$\hat{\Theta}(\phi,\theta) \quad = \quad \arg\max_{(\phi,\theta)} \mathbf{1}^T \hat{\mathbf{R}}_{\phi,\theta} \mathbf{1}, \qquad (7)$$

where the quantity $\hat{\mathbf{R}}$ is an estimate of the correlation matrix of the beamformer output evaluated across a window of length L. The estimator as given by Equation (7) is straightforward to implement in practice and takes only L multiplications and $L-1$ additions to be computed at each (ϕ,θ) iteration. By using the beamforming technique, a significant SNR gain can be achieved with supplementary benefits. For instance, in the presence of a single source, and assuming the free field propagation case, the sound pressure falls off as $1/r$, where r is the range. In the case of four sensors with coherent averaging, the sound pressure becomes four times as large. The noise component will also increase, but only with $\sqrt{4} = 2$ (averaging of power), resulting therefore in an array gain of $\mathrm{AG}_{\mathrm{dB}} = 10\log\left(4/2\right) = 3$ dB. This means that, under spatially distributed white background noise, an array of $M = 4$ microphones would provide an increase in the voltage SNR by a factor of 2 (Ramos et al., 2011). That would be the same as if the sound pressure fell off with $2/r = 1/(r/2)$, and is therefore equivalent to doubling the detection range (Trees, 2002). Moreover, the improved SNR signal at the array's output can be used for features recognition purpose, thereby contributing to lowering false alarm and miss-detection rates.

CONCLUSION

The firing of a gun generates signatures in the acoustic and electromagnetic infrared spectra that can be used to estimate the location of a sniper. The position of the sniper can be estimated if both the ballistic shockwave and muzzle blast acoustic signatures are detected, or by using a laser range finder in combination with infrared signatures or visible light signals reflected from snipers tools. Reliability and robustness are two fundamental requirements of such a system. It is expected that, when deployed, these systems should be able to exhibit a satisfactory performance under adverse conditions involving low SNR and multipath propagation. More robust acoustic sniper localization systems can be developed based on propagation models of both the muzzle blast and the shockwave. In addition, specific problems related to the processing of the signals of interest should also be considered, namely direction-of-arrival (DOA) estimation, noise cancellation, and the multipath propagation effect.

Further developments should address issues such as performance analysis of features recognition techniques in noisy environments, multiple shots and multiple shooters, and exploit the idea of hybrid systems by combining different technologies. System integration to support decision making, specially in cases where immediate engagement might be considered is also worth considering.

REFERENCES

Baker, W. E. (1973). *Explosions in air*. Texas, USA: University of Texas Press.

BBN Technologies. (n.d.). *Raytheon, Boomerang Shooter Detection System.* `http://www.bbn.com`. (Accessed October 15, 2013)

Beck, S. D., Nakasone, H., & Marr, K. W. (2011a, 31 October–4 November). An introduction to forensic gunshot acoustics. In *162nd meeting of the acoustical society of america.* San Diego, California.

Beck, S. D., Nakasone, H., & Marr, K. W. (2011b, April). Variations in recorded acoustic gunshot waveforms

generated by small firearms. *Journal of the Acoustical Society of America*, *129*(4), 1748-1759. doi: 10.1121/1.3557045

Ben-Dor, G., Elperin, T., Li, H., & Vasiliev, E. (1999, May). The influence of the downstream pressure on the shock wave reflection phenomenon in steady flows. *Journal of Fluid Mechanics*, *386*, 213-232.

Brown, J. L. (2011). *High pressure hugoniot measurements in solids using mach reflections* (Unpublished doctoral dissertation). California Institute of Technology.

Brustad, B. M., & Freytag, J. C. (2005, July). A survey of audio forensic gunshot investigations. In *Audio engineering society 26th international conference: Audio forensics in the digital age.*

DuMond, J. W. M., Cohen, E. R., Panofsky, W. K. H., & Deeds, E. (1946). A determination of the wave forms and laws of propagation and dissipation of ballistic shock waves. *Journal of the Acoustical Society of America*, *18*(1), 97-118. doi: 10.1121/1.1916347

Evans, N., Mason, J. S. D., Liu, W., & Fauve, B. (2006, May). An assessment on the fundamental limitations of spectral subtraction. In *Acoustics, speech and signal processing, proceedings of the 2006 ieee international conference on* (Vol. 1, p. I - 145-148). doi: 10.1109/ICASSP.2006.1659978

Jiang, Z., Huang, Y., & Takayama, K. (2004, July). Shocked flows induced by supersonic projectiles moving in tubes. *Computers & Fluids*, *33*(7), 953-966. doi: 10.1016/S0045-7930(03)00041-0

Kastek, M., Dulski, R., Trzaskawka, P., Sosnowski, T., & Madura, H. (2010). Concept of infrared sensor module for sniper detection system. In *Infrared millimeter and terahertz waves (irmmw-thz), 2010 35th international conference on* (p. 1-2). doi: 10.1109/ICIMW.2010.5612447

Mach, E. (1878). Über den Verlauf der Funkenwellen in der Ebene und im Räume (On the propagation of radio waves in the plane and in space). *Vienna Acad. Sitzungsbr.*, *78*, 819-838.

Maher, R. C. (2007, April). Acoustical characterization of gunshots. In *Safe '07: Ieee workshop on signal processing applications for public security and forensics* (p. 109-113).

Maher, R. C., & Shaw, S. R. (2008, June). Deciphering gunshot recordings. In *Audio engineering society 33rd international conference: Audio forensics - theory and practice.*

Plaster, J. L. (2006). *The ultimate sniper: An advanced training manual for military and police snipers* (Second ed.). Boulder, Colorado, USA: Paladin Press.

Ramos, A. L. L., Holm, S., Gudvangen, S., & Otterlei, R. (2011, May). Delay-and-sum beamforming for direction of arrival estimation applied to gunshot acoustics. In *Proc. spie, sensors, and command, control, communications, and intelligence (c3i) technologies for homeland security and homeland defense x* (Vol. 8019, p. 80190U 1-9).

Ramos, A. L. L., Holm, S., Gudvangen, S., & Otterlei, R. (2012, May). Real-time vehicle noise cancellation techniques for gunshot acoustics. In *Proc. spie, sensors, and command, control, communications, and intelligence (c3i) technologies for homeland security and homeland defense xi* (Vol. 8359, p. 835917-835917-9).

Ramos, A. L. L., Holm, S., Gudvangen, S., & Otterlei, R. (2013a, June). A multi-band spectral subtraction based algorithm for real-time noise cancellation applied to gunshot acoustics. In *Proc. spie, sensors, and command, control, communications, and intelligence (c3i) technologies for homeland security and homeland defense xii* (Vol. 8711, p. 871109). doi: 10.1117/12.2018589

Ramos, A. L. L., Holm, S., Gudvangen, S., & Otterlei, R. (2013b, June). The multipath propagation effect in gunshot acoustics and its impact on the design of sniper positioning systems. In *Proc. spie, sensors, and command, control, communications, and intelligence (c3i) technologies for homeland security and homeland defense xii* (Vol. 8711, p. 87110A). doi: 10.1117/12.2018739

Ramos, A. L. L., Holm, S., Gudvangen, S., & Otterlei, R. (2013c, April). A spectral subtraction based algorithm for real-time noise cancellation with application to gunshot acoustics. *International Journal of Electronics and Telecommunications*, *59*(1), 93-98.

Ramos, A. L. L., & Werner, S. (2009, March). QRD-RLS Adaptive Filtering. In J. A. Apolinário Jr. (Ed.), *QRD-RLS Adaptive Filtering* (First ed., p. 147-180). New York: Springer.

REDOWL. (n.d.). *iRobot*. `http://www.irobot.com`. (Accessed October 15, 2013)

Semenov, A. N., Berezkina, M. K., & Krassovskaya, I. V. (2012, July). Classification of pseudo-steady shock wave reflection types. *Shock Waves*, *22*, 307-316. doi: 10.1007/s00193-012-0373-z

ShotSpotter. (n.d.). *SST, Inc.* `http://www.shotspotter.com`. (Accessed December 30, 2013)

Trees, H. L. V. (2002). *Optimum array processing (part iv of detection, estimation, and modulation theory)* (First ed.). New York: Wiley-Interscience.

WeaponWatch. (n.d.). *Radiance technologies.* `http://www.radiancetech.com`. (Accessed October 15, 2013)

Zhang, B., Liu, H., Chen, F., & Wang, G. (2012, July). Numerical simulation of flow fields induced by a supersonic projectile moving in tubes. *Shock Waves*, *22*, 417-425. doi: 10.1007/s00193-012-0389-4